# Moho topography under central Greece and its compensation by Pn time-terms for the accurate location of hypocenters: The example of the Gulf of Corinth 1995 Aigion earthquake

M. Sachpazi [a,*], A. Galvé [b], M. Laigle [b], A. Hirn [b], E. Sokos [c], A. Serpetsidaki [c], J.-M. Marthelot [d], J.M. Pi Alperin [d], B. Zelt [e], B. Taylor [e]

[a] Geodynamical Institute, National Observatory of Athens, Greece
[b] Laboratoire de Sismologie Expérimentale, UMR 7580 Dpt de Sismologie, Institut de Physique du Globe de Paris, France
[c] University of Patras, Greece
[d] Ecole et Observatoire, Institut de Physique du Globe de Strasbourg, France
[e] University of Hawaii, United States

## Abstract

In this paper we expand over the whole of central Greece, the Moho map centered on the Gulf of Corinth from tomographic inversion of PmP traveltime profile data recorded by several tens of temporary stations. Our approach is based on Pn, Moho refracted waves, from a large regional earthquake recorded by both temporary stations and the permanent Hellenic network. The Moho map shows the large Moho depth under the Hellenides belt. It also highlights the shallower Moho domain towards the Aegean Sea south and east of the Corinth Gulf. The domain of shallow Moho is limited along a NE–SW prolongation ahead of the North Anatolian Fault, from the North Aegean Trough to the western tip of the Gulf of Corinth towards the Gulf of Patras. The Pn time-terms provide corrections for the permanent stations that can be used together with the 1D velocity–depth model for a first-order compensation of lateral heterogeneity and contribute to the accurate and fast location of earthquake hypocenters. As a test we relocated the 1995 Aigion earthquake in this way, using only the sparse data of the permanent stations. Hypocentral coordinates then shift close to those derived by a dedicated dense array deployed after the earthquake, implying improvement of the routine location.
© 2007 Elsevier B.V. All rights reserved.

## 1. Introduction

The structure of the lithosphere in Greece has been the subject of numerous studies using a range of seismic methods, among which, pioneering artificial source studies (Makris, 1978). In the last thirty years however, crustal thickness and velocity–depth function from the surface into the mantle, as well as their variations throughout Greece, have not been investigated with the high

---

\* Corresponding author.
  *E-mail addresses:* m.sachp@gein.noa.gr (M. Sachpazi),
galve@ipgp.jussieu.fr (A. Galvé), laigle@ipgp.jussieu.fr (M. Laigle),
hirn@ipgp.jussieu.fr (A. Hirn), esokos@upatras.gr (E. Sokos),
annaserp@upatras.gr (A. Serpetsidaki), jmm@eost.u-strasbg.fr
(J.-M. Marthelot), taylorb@hawaii.edu (B. Taylor).

resolution provided by artificial source refraction–reflection surveys, apart from some sampling of the marine domain (Hirn et al., 1996; Sachpazi et al., 1997; Clément et al., 2000; Vigner, 2002).

Several seismological techniques have been used in the region. Teleseismic or regional earthquake body wave delay-time tomography (Spakman et al., 1993; Papazachos and Nolet, 1997) and surface wave tomography (Karagianni et al., 2005) have contributed to a knowledge of the large-scale general structure. However these studies do not have fine lateral or depth resolution in the upper layers lacking ray-crossing, due to the loose spacing of permanent seismological stations. Teleseismic tomography with denser temporary profiles of receivers (Tiberi et al., 2001) still lack depth resolution at the crust–mantle boundary depth range and provide only indirect evidence of the Moho boundary. In contrast, the Moho can appear by an identifiable signal from bottom-side P to S interface conversion in transmission by the teleseismic receiver-function method. The latter has however a limited resolution in depth due to the low frequency of large distant earthquakes, the limited constraints on the P and S slowness and also to the sparse horizontal spatial sampling by the few permanent stations.

The Moho was detected at 42 km depth under the western tip of the Gulf Of Corinth and at 36 km depth north of its eastern part, by PmP wide-angle reflections (Clément et al., 2004). These PmP data were obtained at two land stations that recorded the axial profile shot from the N/O NADIR in single-bubble mode with a 14 air-gun array of 2600 cu. in. during the 1997 SEISGREECE cruise (Sachpazi et al., 1997; Clément et al., 2000; Clément et al., 2004). These Moho depths are over 5 km larger than published results for the thinned crust in the Aegean domain, such as the Moho depth map from gravity inversion referenced to teleseismic tomography of Tiberi et al. (2001).

Such large values of absolute Moho depth, as well as crustal thickness variations amounting to 20% over less than 100 km distance, have been confirmed and expanded recently from the 2001 cruise EW-0108 of R/V Maurice Ewing in the Gulf of Corinth. Multichannel reflection seismics were carried out in the Gulf of Corinth in 2001, with a 20 air-gun array source of 8000 cu. in. recorded by 240 channels along a 6 km streamer and also several tens of stations onshore over Greece. Zelt et al. (2005) inverted in 3D the crustal thickness and velocity variations using the PmP wide-angle Moho reflections of the numerous shot-lines at sea recorded on land. The arrival times of the PmP Moho reflections could be accurately compensated for propagation through the sedimentary infill imaged reliably by MCS under the shot lines (Zelt et al., 2004). They resulted in a high-resolution map of the Moho topography centered on the Gulf, that will be complemented by the present study and presented jointly in Fig. 5.

The crustal structure results of such dedicated surveys have the potential to improve the reliability and accuracy of earthquake locations from the permanent seismological stations, in a seismicaly active region. In Greece, seismicity is widespread and thus a very large amount of permanent stations would be necessary to ensure good constraints on location and depth everywhere. For earthquakes that are not inside the network, the location of the epicenter shifts with the geometry of the network and the velocity model. In case of large variations of Moho topography as can be expected here, this is even worse. Thus, the knowledge of the Moho topography as well as of the velocity–depth model is a key-point to the problem of reliable and fast location of earthquakes. The latter is important for Civil Defence for the understanding of the phenomenon and its possible evolution and is crucial for deployment of the aftershock recording array.

In this paper we extend over central Greece the Moho map, centered on the Corinth Gulf, obtained by Zelt et al. (2005) from the inversion of PmP traveltime data from marine airgun shot profiles in the Gulf recorded on temporary land receivers. Our approach is based on Pn, Moho refracted waves from a large earthquake observed by these several tens of temporary stations and permanent ones. This allows us to extend the sampling of the lateral variation of the crust. Large crustal thickness variations are revealed.

The Pn time-terms we determined, provide station corrections that may be used together with the 1D velocity–depth model for a first-order compensation of lateral heterogeneity. Relocation of the 1995 Aigion earthquake in this way, using only the sparse data of the Hellenic permanent monitoring array available in real-time, shifts the hypocentral parameters closer to those obtained by relocation derived with the data of several weeks of aftershocks recorded by a dense local array deployed after the mainshock (Bernard et al., 1997).

## 2. Sampling Moho depth variations from Pn arrival times of the same earthquake at a dense regional array

Crustal thickness and its spatial variation are generally inferred indirectly from observations that are not those of the original Moho diagnostic wave. Indeed, the most reliable way to identify the crust–mantle boundary, or Moho, but also to determine accurately its depth, and image its lateral variation is by using the Pn wave, as it was originally defined (Mohorovičić, 1910). This is a first

arrival, hence unambiguously identifiable, from hundred kilometers range where it has overtaken waves propagated in the crust, to several hundred kilometers distance. This Pn wave has, however, a low amplitude being an interface head-wave and artificial source seismics can excite it only at the expense of very strong sources. On the other hand natural earthquake sources with large magnitudes may also provide large Pn signal amplitude. Here we will use the Pn wave from a strong regional earthquake to map the variation of Moho depth under central Greece.

We use data of a 40 receivers temporary array which had been deployed over central Greece during Cruise EW-0108 of R/V Maurice Ewing (Taylor et al., 2003) in order to record shots used by Zelt et al. (2005). The same array (Fig. 1) recorded a Mw=6.4 earthquake near Skyros island in the north central Aegean Sea on 26 July 2001 (e.g. Papadopoulos et al., 2002; Ganas et al., 2005).

The mainshock and two strong aftershocks were also recorded by 40 geophone groups on land spread along 8 km long and by the 240-channel, 6 km long recording streamer cable of the R/V Maurice Ewing. Data of the permanent seismological stations of the National Observatory of Athens (NOA) and of the University of Patras (PATNET) have also been added to the dataset, giving an unprecedented spatial sampling. These different arrays, each of a homogeneous instrument type, but different from each other are tied together by some common locations with the temporary array. The waveforms of the temporary receivers with 4.5 Hz natural frequency sensors were corrected for instrument response in order to be able to compare waveforms of the long duration source of this large earthquake with the waveforms recorded by the broad-band or by the 1 Hz sensors of the NOA and PATNET arrays. Then considering this earthquake at
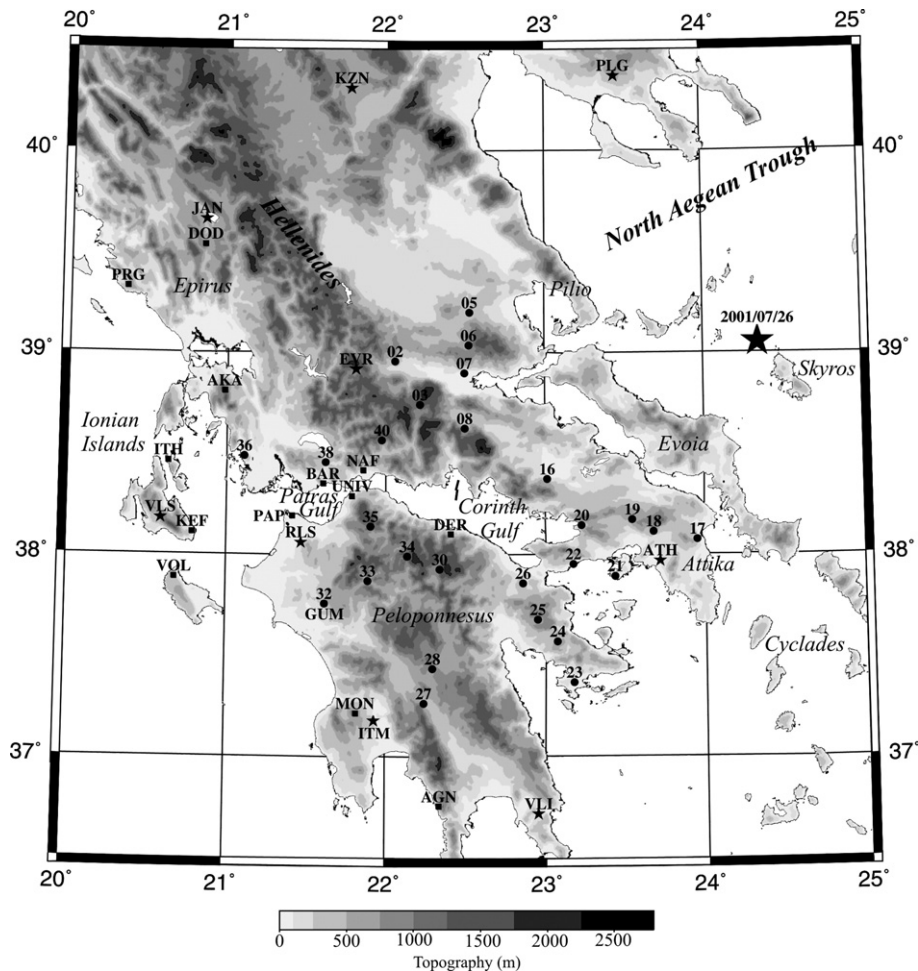


Fig. 1. Map of Greece with location of Skyros epicenter, temporary stations (dots), NOA-Athens (stars) and University of Patras (squares) permanent seismometers. The two lines in the Gulf of Itea in the Corinth Gulf are the successive locations of the recording streamer of R/V Maurice Ewing during the mainshock and its first largest aftershock.
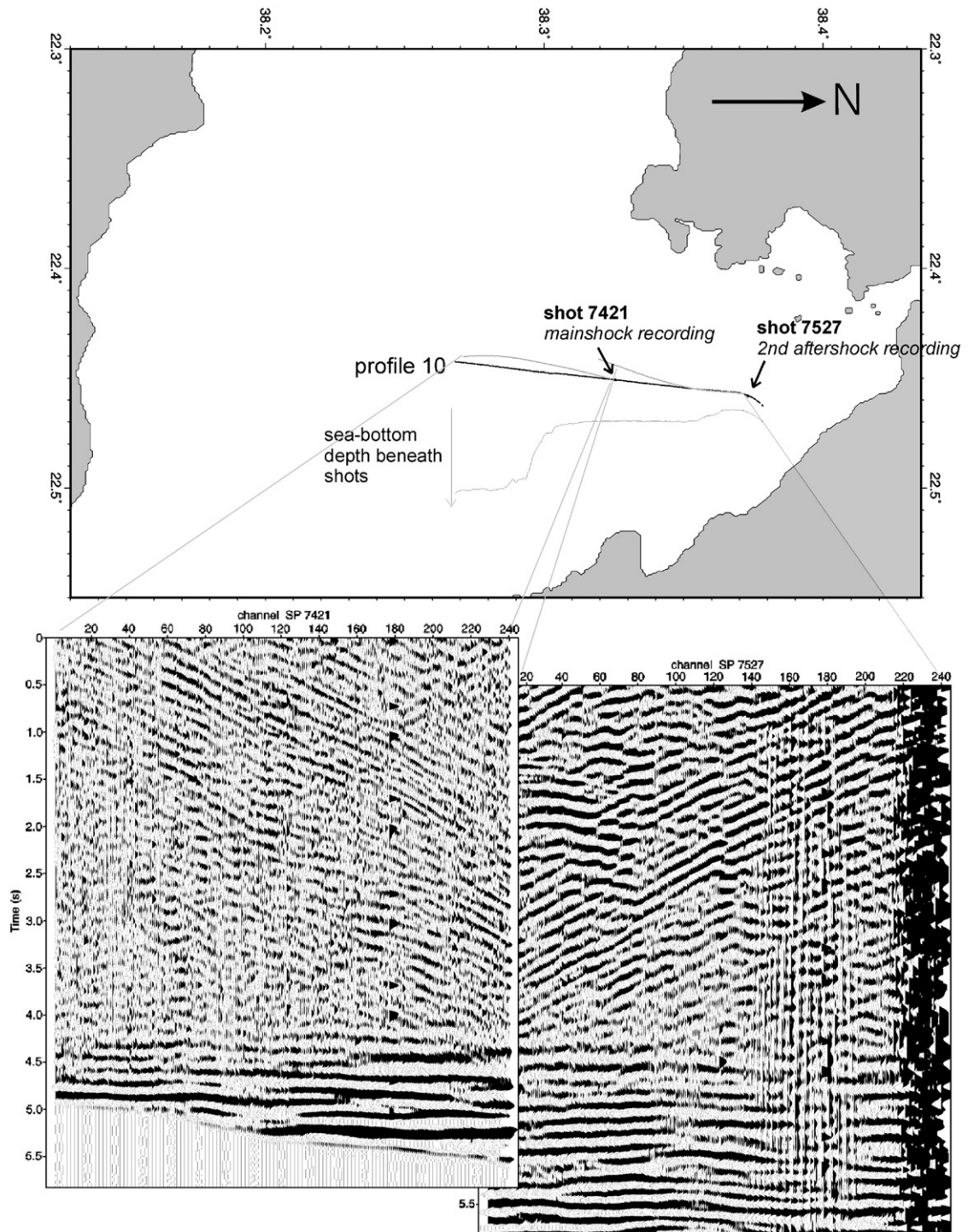
Fig. 2. Marine seismic "streamer" recording in the Gulf of Itea (Fig. 1). Profile of total length of 10 km with hydrophone receiver groups at 25 m interval, composite of record of mainshock and first main afershock recorded by two successive positions of 240 channels 6 km long streamer with some overlap. Source gather plotted with reduced-time vs. distance, i.e. linear moveout corrected for 8.0 km/s refraction velocity. Basement statics are applied, that is times have been corrected for water depth and structure above basement as inferred by Zelt et al. (2005) from tomography on the streamer along that profile.
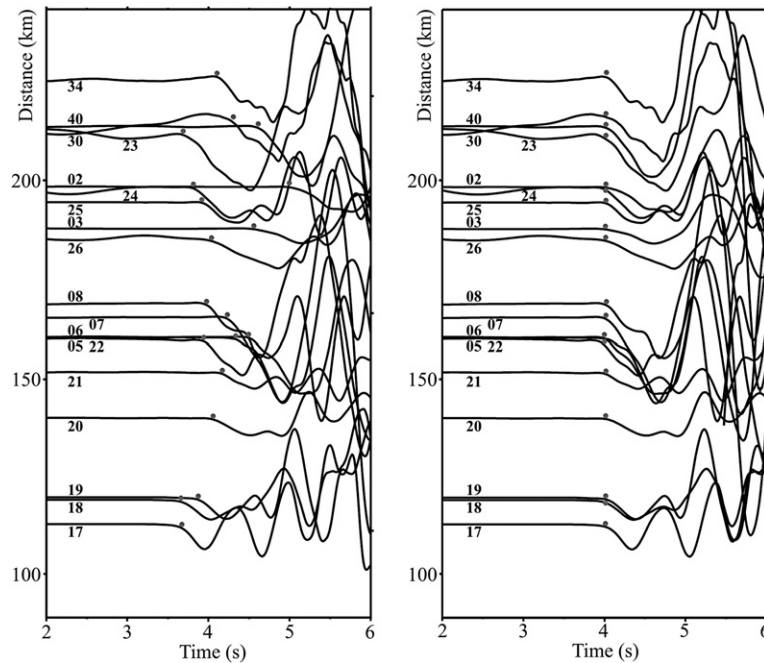
Fig. 3. Examples of waveforms recorded on temporary receivers. (a) As a function of distance, source gather plotted with reduced-time vs. distance, i.e. linear moveout corrected for 8.0 km/s refraction velocity. (b) Waveforms time-shifted in order to align on the 8.0 km/s velocity. These time-term variations are used to map Moho depth variation in Fig. 5.

several stations, high-resolution differential time picking to 0.01 s is reached by cross-correlation or eye-fitting of superimposed waveforms.

The Pn wave propagates beneath and along the Moho at a velocity on the order of 8 km/s. Waveforms are displayed in Figs. 2, 3 and 4 in reduced time or delay-time with respect to a wave propagating at this velocity. If crustal thickness and velocity, as well as mantle velocity were the same for the whole region, waveforms of all receivers should be at the same reduced time, which is clearly not the case since they spread over one second around it. These variations of delay-times among receivers are controlled mainly by variations in Moho depth. For example for an average crustal velocity of 6.25 km/s (Zelt et al., 2005), with a 8 km/s mantle velocity, the variation in the receiver delay-time $\tau$ in seconds with differential Moho depth ($H$) in kilometers is $\tau(s) = 0.1H$ (km). Moho depth variations of over 10 km likely can explain such delays. The influence of reasonable variations of other parameters is smaller. For example the depth of the intracrustal interfaces assumed in our model (a 6.0 km/s upper crustal layer and a 6.75 km/s lower one) may also vary but its effect would be of an order of magnitude smaller than Moho topography, due to the much smaller velocity contrast across them. Hence their influence is not taken into account. The sensitivity of Pn delay-time to possible changes in average crustal velocity under receivers is also much smaller. Variations of up to

0.2 km/s (from 6.2 to 6.4 km/s) would result in only 0.03 s change in the time-term. The average velocity may also vary strongly laterally by possible low-velocity layers in the crust. However, as shown by Papazachos and Nolet (1997) such features exist principally to the west of our study area.

In Fig. 3, waveforms are plotted at reduced times as a function of distance. We observe that their delay-times
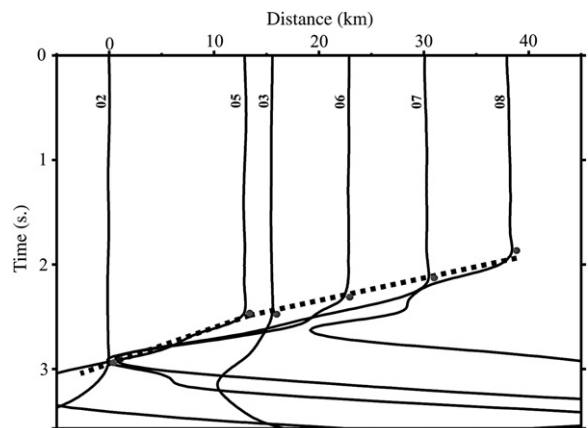


Fig. 4. Waveforms obtained at receivers northwest of the eastern Gulf of Corinth projected along fan profile. Sources gather plotted with reduced-time vs. distance, i.e. linear moveout correction for 8.0 km/s refraction velocity. Distances on horizontal axis are along fan profile.

scatter without any trend with distance. This indicates that other values than 8 km/s for the mantle are not better on average and we would have to switch back and forth between values of 7.2 and 8.8 km/s over distances of some kilometers along the profile of stations. This would not even account really for the scatter, since even for receivers at the same distance as for example at 160 km the waveforms are shifted (Fig. 3). This is also indicated in Fig. 4 by the plot of waveforms of neighboring stations that form a kind of fan-profile not differing much in distance from the source, in an approximate NW–SE section along the strong Moho variation centered at 39 °N 23 °E. Therefore it is not likely that for these rays that leave the source in a tight range of azimuth, the cause for the time delays is different mantle velocities. Thus, at first order the variation of delay-times appears to be controlled by variations of Moho depth.

## 3. Moho topography approached by Pn time-terms

The propagation time, from a source $S$ to a receiver $R_i$ at distance $D_i$, of a wave refracted at a horizon with velocity $V_m$, here the mantle velocity, may be written as:

$$T(S, R_i) = \tau(R_i) + \tau(S) + \frac{D_i}{V_m} \quad (1)$$

with $\tau(R_i)$ and $\tau(S)$ being the receiver and source time-terms (e.g. Willmore and Bancroft, 1960).

What is known, is the arrival times $T(S, R_i)$ among a set of receivers $R_i$, as well as an independently derived estimate of the location of the earthquake source. Assuming the reliability of its coordinates in the horizontal plane, we get the epicentral distances $D_i$. The estimates of the other parameters of the earthquake source, focal depth and origin time, trade off among themselves and also with both the difference between the true Moho depth under the source and that assumed in the location routine. In our case though, we work with arrival time differences between receivers from a same source. Thus, these less reliably determined parameters simplify out of the relations as part of the source time-term.

For a horizontal marker refractor, the time-terms are simply the refraction intercept times, that is

$$\tau(R_i) = H(R_i) \cdot \frac{\cos\theta_c}{V_c} \quad (2)$$

with $\sin\theta_c = \frac{V_c}{V_m}$ the ratio of velocities of the overburden, here the crust, $V_c$, to the mantle, $V_m$; and $H(R_i)$ being the perpendicular from the receiver to the marker. As a first approximation, the differences in marker depth beneath receivers with small differences in time-terms can be

approached by this relation that is valid for the case of small dips.

We consider here the more general relation for the propagation times in the case of an inclined raypath under a refractor marker with dipping sides under the source $S$ and the receiver $R_i$ (Willmore and Bancroft, 1960). We assume though for simplicity that the refractor dip is the same under source and receiver, $\alpha_i$.

Eq. (1) can also be written as:

$$T(S, R_i) = \frac{H(R_i) \cdot \cos\theta_c}{V_c} + \frac{H(S) \cdot \cos\theta_c}{V_c} + \frac{D_i \cdot \cos\alpha_i}{V_m} \quad (3)$$

where the crustal velocity $V_c$ is taken as 6.25 km/s, $V_m$ a standard mantle velocity of 8 km/s and $H(S)$ is the perpendicular from the source to the marker.

However the values we deduced from Fig. 3, are traveltime terms $t(S, R_i)$ at a reduction velocity of $V_m$ and therefore from relation (3), we have

$$t(S, R_i) + \frac{D_i}{V_m} = \frac{H(R_i) \cdot \cos\theta_c}{V_c} + \frac{H(S) \cdot \cos\theta_c}{V_c} + \frac{D_i \cdot \cos\alpha_i}{V_m} \quad (4)$$

The focal depth of the Skyros earthquake is not well constrained, but we can omit the corresponding $H(S)$ by using the traveltime difference between two receivers $R_i$. This allows us to deduce the difference in depths under them $\Delta H(R_i)$. However, to calculate the absolute value $H(R_i)$, we need to have one or several references points $H(R_a)$ that we are going to deduce from the Moho map of Zelt et al. (2005), where several receiver positions are common with the present study.

Let us assume two receivers $R_2$ and $R_1$. From relation (4), the traveltime difference between the two receivers allows us to deduce the depth variation as:

$$H(R_2) - H(R_1) = \frac{V_c}{\cos\theta_1} [t(S, R_2) - t(S, R_1)] - \frac{V_c}{\cos\theta_1} \left[ \frac{(D_2\cos\alpha_2 - D_1\cos\alpha_1)}{V_m} - \frac{(D_2 - D_1)}{V_m} \right] \quad (5)$$

We can easily calculate the first term on the right-hand side, and for the second we have to estimate first the dip $\alpha_i$, for which as mentioned we consider in a first approximation that it is the same on the source and

station side. Since the Skyros earthquake occurred in the region between the North Aegean Trough and the Cyclades Plateau where Moho is at 25 km depth (Vigner, 2002), we introduce this value to compute these

$$\alpha_i = \arcsin\left(\frac{25 - H(R_i)}{D_i}\right) \tag{6}$$

However the depth $H(R_i)$, that is at the perpendicular from the receiver to the dipping refractor is not sampled by the ray, since the ray pierces the Moho at a horizontal distance $d(R_i)$ before the receiver in its way upwards, which is several tens of kilometers. Thus, the Moho piercing point is determined by $d(R_i)$ and $hR(i)$ where $d(R_i)$ is the distance between the piercing point and the receiver and $hR(i)$ its depth.

$$d(R_i) = \frac{H(R_i) \cdot \sin(\theta_c + \alpha_i)}{\cos\theta_c} \tag{7}$$

$$h(R_i) = \frac{H(R_i) \cdot \cos(\theta_c + \alpha_i)}{\cos\theta_c} \tag{8}$$

We first estimate $R_a$ for stations for which piercing points from the Moho are inside the region sampled by Zelt et al. (2005). In this way we tie the Moho depth variations among receivers $R_i$, to the absolute Moho depth in the region of the Gulf of Corinth. We focus on stations which sample the central part of the Corinth Gulf, where there is no large and rapid changes in Moho depth. For these stations we estimate the depth of their Moho piercing point $h(R_a)$. From this, we can estimate the Moho interface dip $\alpha_a$ between the station $R_a$ and the source $S$, as well as the depth $H(R_a)$ using relation (8).

After that, from the differences of time-term between receiver $R_a$ and $R_i$ and the now known value of $H(R_a)$, we can estimate $\alpha_i$, then $H(R_i)$ and finally $h(R_i)$ and $d(R_i)$. This procedure is repeated for each couple of receivers.

In Fig. 5 the resulting Moho piercing points and corresponding depths are plotted and contoured to produce a map of Moho topography, the central part of which has been taken from the study of Zelt et al. (2005).

To the north-west of the Gulf of Corinth, the large Moho depth obtained towards the edge of the map of Zelt et al. (2005) is confirmed, and documented here to extend northward towards Epirus, along the strike of the Hellenides mountain belt, with maximum depths over 50 km. The thick crust is attested by data obtained from the westernmost receivers of the temporary array and from the permanent stations in Epirus.

From permanent stations on the Ionian islands, the estimated Moho depths under the western gulf of Patras

indicate that the Moho is less than 45 km deep there. The obtained values may still overestimate the true depths and carry a delay from Pn diving under the Hellenides before rising towards the west. Hence, these points have not been included in the contouring of Moho depth.

To the south of the western gulf of Corinth our results confirm the rather steep gradient of a deep, over 40 km depth, Moho, opposed to a shallower Moho with depths of over 30 km, estimated for the eastern edge of Peloponnesus. These features can now be extended southwards from data obtained by the temporary and permanent stations in southern and western Peloponnesus.

To the east, the region of shallower Moho under the eastern gulf of Corinth of Zelt et al. (2005) extends southeastward into Attiki and after reaching locally a depth larger than 30–33 km, Moho gets shallower again, reaching less than 30 km depth towards the Aegean Sea, in Evvia Island.

The domain of shallow Moho shows a strong contrast with the deeper domain to the NW, and is limited by a NE–SW striking feature across which the Moho shows a strong gradient or step in a depth. This is documented by receivers located far north of the Gulf spreading as a kind of fan profile (Fig. 4). Along this NE–SW striking trend the 35 km Moho contour is shifted right-laterally by 80–140 km distance from the tip of the Magnesian peninsula SW of the North Aegean Trough to the Hellenides belt in the Peloponnesus, south of the Gulf of Corinth. Thus, the results reveal the expression of a through going feature at the Moho level and crustal scale. The existence of such feature has been debated, after the early proposal of McKenzie (1972) of a right-lateral transform plate boundary between the North Anatolian Fault and the western Gulf of Corinth or Patras and Kefalonia Island, due to lacking continuity in the surface geology observations. At this stage, this observation is an incitation to submit this question to further investigation, rather than a definite proof.

## 4. Moho refracted and direct crustal waves for locating local–regional earthquake hypocenters from sparse arrays of permanent seismic stations

Under the assumptions of regionally constant average crust and mantle velocities, we computed the time-terms of the receivers as a function of hypocenter–receiver position for their Moho piercing points. This provides the station corrections, that we introduced to the Pn arrival time readings in the location routine together with the assumed 1D velocity–depth model. The location of other earthquakes can thus be computed
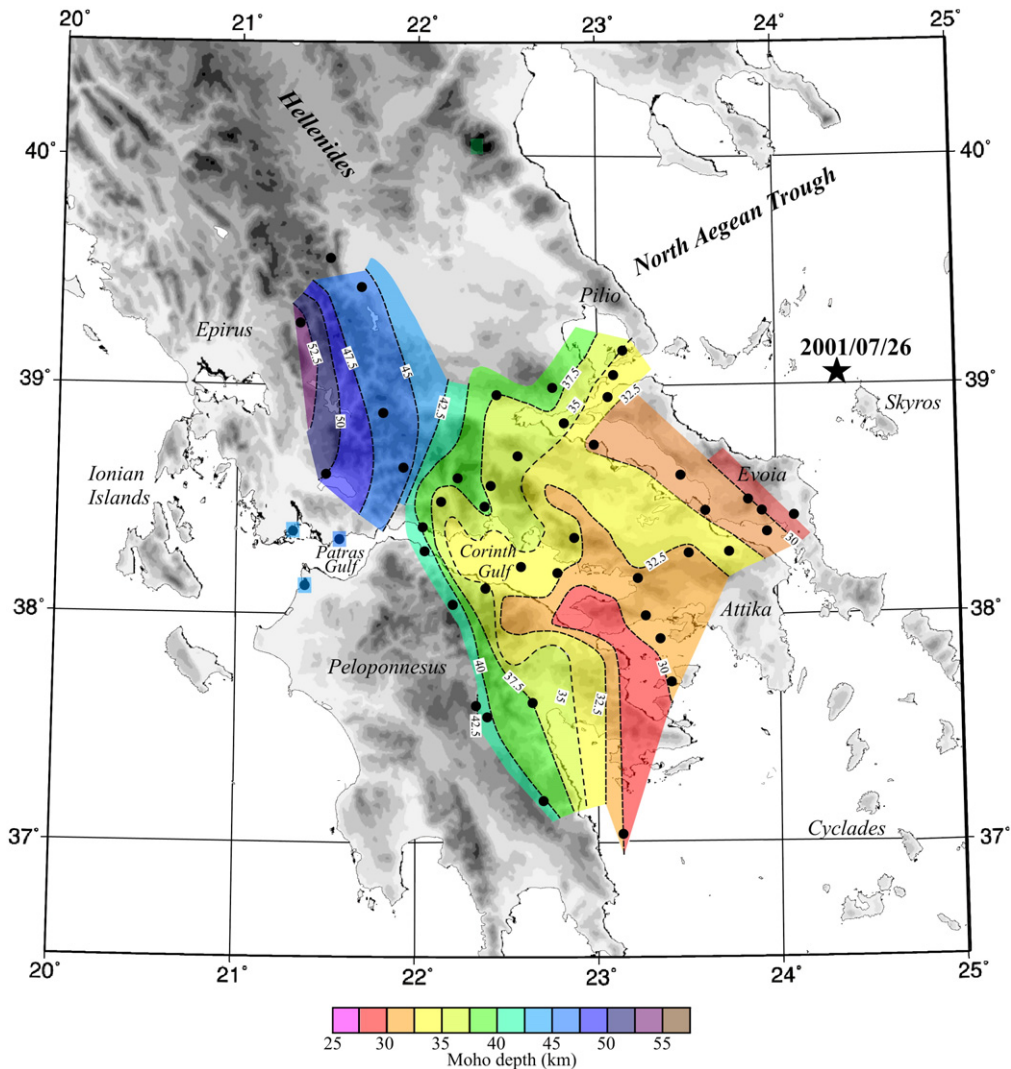
Fig. 5. Moho topography in central Greece, derived from station Pn time-terms from the Skyros earthquake at data points (dots), tied in with the Moho depth map of Zelt et al. (2005) obtained from tomographic inversion of PmP. Depth variations are computed in the case of laterally constant average 6.25 km/s crustal and 8 km/s mantle velocities. Lateral decrease or increase in crust or mantle velocity would induce corresponding variations of Moho depth as described in text. Specific depth value estimate is only an upper bound in case of downdipping Moho from the Corinth region, as in the NW Hellenides.

by taking into account the spatial variation of the Moho depth among receivers. In the next section we will apply this procedure to the case of the 1995 earthquake of Aigion that occurred in the western part of the gulf which is well imaged by both PmP and Pn data. The source side time-term variation for the different azimuths towards each recording station is derived from our Moho map. For stations that gave stand-alone observations being in northern Greece or in the Aegean we consider the time-terms derived from the Skyros earthquake. We make this assumption because the stations are far from both the well resolved by the Skyros earthquake data region, and the Aigion earthquake

region. Therefore the piercing points of the rays towards the station are close enough to consider the time-term derived from the Skyros earthquake. The resulting correction that compensates the observed times for the lateral Moho depth variation near to source and receiver ranges over 1.5 s among the recording stations.

The 1995.06.15, Ms=6.2 Aigion event has been located diversely by national or international agencies and has been a topic of research (Tselentis et al., 1996; Bernard et al., 1997). New images of the deep structure across the Gulf of Corinth by multichannel reflection seismics and OBS refraction revealed the existence of a north-dipping low-angle normal fault. The fault cuts the

pre-rift basement and links, to form a bi-planar fault, with a steeper segment outcropping at the south coast of the Gulf (Clément et al., 2004). Sachpazi et al. (2003) proposed a seismo-tectonic interpretation of this earthquake with respect to the deep structure and discussed its implications in terms of the behavior of active normal faults. This joint interpretation is plausible with the hypocenter location of Bernard et al. (1997) who report a north-dipping low-angle fault plane solution consistently with GPS and INSAR modeling. The other estimates of the hypocenter, under the northern coast or the center of the gulf obtained from various permanent Greek arrays, or much further away obtained by international agencies from worldwide data, are 10 km deeper than the discovered bi-planar fault.

From the PmP inversion of Moho depth by Zelt et al. (2005), it appears now that this earthquake has its source above a major lateral change in Moho depth. This has implications on the estimation of its location, by regional networks, since this 3D Moho variation is not taken into account in the studies that use the 1D assumption of structure. Previous attempts to take into account lateral heterogeneity have been made using various estimations of station corrections (e.g. Panagiotopoulos and Papazachos, 1985). In these earthquake location studies the assumed average Moho depth, as well as the velocities in the upper and lower crust are very different from each other and from the ones we calculate. Furthermore, among those studies, the sets of observations used are also fundamentally different.

In continental regions earthquakes occur in the upper crust, and there is a trade-off between the computed focal depth and the Moho depth assumed for the computation. This is because these moderate earthquakes are commonly detected only by the seismological stations of permanent regional arrays recording in the few hundred kilometers range. First arrivals change from crustal Pg to mantle Pn wave types at distances between 100 and 200 km depending on both Moho and hypocenter depths. The first-arrival time picks then distribute between two very different subsets: Pg at the shorter range that have up-going rays from the hypocenter and Pn, that have the down-going ray from the hypocenter to the Moho and then refracted to larger distances. The computed focal depths depend on the assumed value of Moho-depth, with larger values resulting in larger focal depths. When Pg are not obtained with the same azimuthal distribution as Pn, the trade-off affects the epicentral coordinates as well.

Other parameters of importance in addition to the average Moho depth and crustal velocity are: (i) the velocity change in the crust above and below the hypocenter that also controls the time difference for up- and down-going waves, (ii) the upper mantle velocity, and (iii) the P to S velocity ratio in the case that arrival times of the two waves can be used. Furthermore, in the common location routines using a 1D velocity model, there is the usual effect of neglecting lateral variations of structure. The latter, for the same earthquake, can be summarized as variations, along the hypocenter–station path of: (a) the Moho depth and its variation with azimuth, or the corresponding Pn time-term under the hypocenter with respect to the 1D model, (b) the mantle velocity along the path, (c) the Moho depth at the emerging point for the up-going ray towards the recording station and its variation in respect to the assumed 1D model or the corresponding Pn time-term.

The influence of 1D structural multipathing on the depth determination exists even for a perfect distribution of stations with azimuth and distance. The problem gets worse in the case of a sparse observation array implying an azimuthal gap in coverage. For instance, Papadopoulos et al. (1988) using additional data from temporary stations have shown that epicenters for earthquakes in the Hellenic arc are located tens of kilometers from those estimated by the permanent array.

Thus the geometry of the recording permanent stations is a serious problem because in this case lateral variations of structure may not statistically be compensated as it is expected when observations of many stations are available. Conversely, as we will illustrate, the use of the correct average model and of station corrections derived from structural studies may provide us with accurate hypocenters.

## 5. Implications on the location of earthquakes — case study of the 1995 Aigion earthquake

Bernard et al. (1997) have studied the 1995 Aigion earthquake of Ms = 6.2. They used for the mainshock in addition to the NOA array, the important complement of S–P times at 3 accelerographs at short distance range on both coasts of the Gulf. Furthermore, they located with a fine accuracy the absolute coordinates of the aftershocks with a dense local array. They recovered the absolute coordinates of the mainshock by differential location, with the help of the NOA array recordings of both the mainshock and main aftershocks.

Indeed for this relocation they used principally 2 of the NOA stations that were the closest in the Pg range of hypocenters (RLS and EVR). They also used, but with a lesser weight, the 3 next ones (ITM, VLS and VLI), and discarded the other. In our tests for an absolute location of this earthquake, we have included data from all those

NOA stations that recorded the mainshock (including the corresponding Pn station corrections KZN, −0.75 s; NPS, +0.75 s; PL, −0.25 s, PRK, +0.75 s, RDO, −0.6 s; VAM, +0.85 s, VLI, −0.15 s), to have enough readings for the location routine. In this way, the data of these stations can be accounted for reasonably. However, hypocentral results are influenced by the reading of ATH that is a generally noisy station. In addition, ATH's distance (120–130 km) for this earthquake makes the first arrival wave identification (Pg or Pn) equivocal. Unfortunately it is also the only station that contributes with data for a large span of azimuths and thus corresponding ambiguities may have an unduly large influence on results. For this station, we tested different weights in the Hypo 71 location procedure that is quality up to 3, with the latter giving satisfactory solutions. We consider that unfortunately the results for the case of the Aigion earthquake are only marginally significant since the stability of solutions remains dependant on a priori values of initial hypocenters, and because the azimuth–distance distribution of recording stations is limited.

Bernard et al. (1997) have defined a posteriori their preferred location (red circle numbered 3 in Fig. 7) of the mainshock as 38° 21.7′ N; 22° 12.0 E, depth 10 km. Their location is significantly different from the one given routinely immediately after occurrence by the National Observatory of Athens (NOA) (green dot numbered 2 in Fig. 7), that was 5 km to the NW and 16 km deeper. Bernard et al. (1997) solution is also different from that of PATNET array maintained by the University of Patras (yellow dot numbered 1 in Fig. 7), that was 10 km to the SW, although at the same depth (Tselentis et al., 1996). The above estimates of the hypocenter are 10 km deeper in both cases than the active intracrustal fault imaged by marine reflection seismics (Sachpazi et al., 2003) and thus, preclude any discussion of the relation between reflection derived structure and seismic activity.

A broad range of hypocenter location tests were run with different location routines, with different values of initial hypocenter coordinates, and with a broad range of input models (velocity–depth functions that are displayed in Fig. 6) and data. Main results are plotted in Fig. 7 and can be discussed as follows:

In Fig. 7, the hypocenters labeled N are obtained with the new model and Pn time-term corrections as derived in this study. N1 is, with only (but all) the NOA array readings, N2 with the addition of data of 3 nearby accelerometers, and N3 with addition of the PATNET readings. These hypocenters located close to each other, indicate that the new model and Pn time terms produce similar results using different data sets, that gave dif-
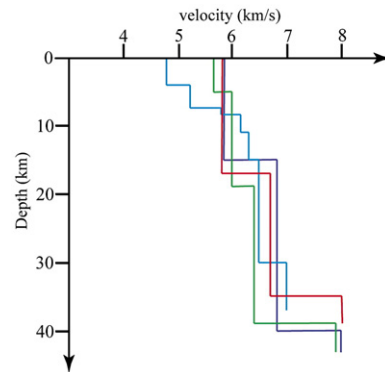


Fig. 6. Velocity–depth functions considered in the re-location of the 1995 Aigion earthquake. Red: model N, preferred model used as deduced from PmP tomography by Zelt et al. for the crust and taking a 8 km/s velocity below Moho. Purple: model O, NOA model, for routine early locations. Green: model used in Tselentis et al. Blue: model R, of Rigo et al. (1996), also used by Bernard et al. (1997).

ferent hypocenter estimates, 1 and 2, in previous studies. These N1, N2, N3 hypocenters are 2 to 4 km to the NNW and 1 to 3 km deeper than the hypocenter of Bernard et al. (1997). Thus, these would plot along the same northward shallow-dipping fault and the discussion of the relation of the hypocenter to the prolongation of the fault documented under the marine part of the Gulf of Corinth from Sachpazi et al. (2003) applies in any case. As mentioned, all NOA data, mostly discarded in the relocation of Bernard et al. (1997) are included here, but ATH still has to be given a lower weight. The solution N1, obtained by only the NOA array data which were available in real-time and the new model is significantly closer to hypocenter 3 than are hypocenters 1 and 2. Instead, the hypocenter obtained for this same set of NOA stations but using the Rigo et al. (1996) 1D model (in blue, Fig. 6) would plot several kilometers to the east, outside the frame of Fig. 7. Also, the hypocenter located by the same set of NOA stations and the NOA model (in purple, Fig. 6), though it has an epicenter close to N1, is 10 km deeper. If we attribute the highest quality for the reading of ATH, since it is the only station for a large span of azimuth, the obtained solutions have too large depth with respect to the likely best estimate of Bernard et al. (1997), numbered 3 in Fig. 7. With the new model and Pn time-terms, it plots at point N in Fig. 7 but at 19 km depth; with the NOA model it plots at point O but at 20 km depth and with the model of Rigo et al. (1996) it plots at point R, but at 26 km depth.

An important result is that even with only the original data of NOA available in real-time, the hypocenter N1 is significantly closer to that of Bernard et al. (1997), numbered 3 in Fig. 7 than other estimates obtained by
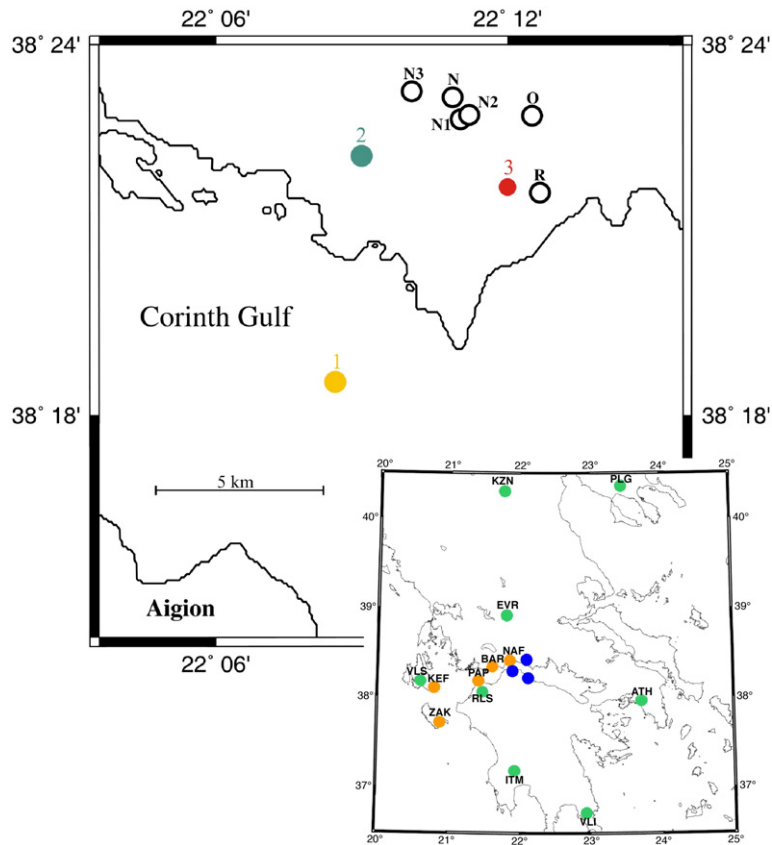
Fig. 7. Inserted map of Greece identifies closest stations used in discussing location of 1995 Aigion earthquake. Green dots: permanent seismographic stations of NOA; brown dots: stations of University of Patras; blue dots: accelerometric stations. Red dot labelled 3 (depth 10 km) is taken as the best estimate of the real hypocenter of the Mw=6.2 Aigion earthquake as obtained by Bernard et al. (1997). Preliminary solutions provided soon after occurrence by agencies using worldwide observations would all plot out of the frame of this Figure. The provisional hypocenter provided by NOA, the Greek national array of the National Observatory of Athens, is indicated by a green dot numbered 2 and is at a 10 km larger depth than the solution of Bernard et al. (1997). Solution obtained with the PATNET regional array (Tselentis et al., 1996) is marked by a yellow dot numbered 1 (depth 10 km). Points labelled N are relocations of the hypocenter by using the new 1D model, consisting of an equal thickness two-layer crust with 6.0 and 6.7 km/s velocities and a 35 km deep Moho, and corrections to arrival time picks corresponding to source and receiver Pn time-terms according to the Moho depth map of Fig. 5. With this model, N1 (depth 13 km) is with only the NOA array data, N2 (depth 12 km) with addition of the 3 readings of the accelerometers also used by Bernard et al. (1997) and N3 (depth 14 km) the same supplemented with readings of the Patras array of Tselentis et al. (1996). The N1, N2 and N3 are obtained with all stations as reported, but a reduced weight for station ATH, of quality 3. With the same array data, but the NOA model, the hypocenter would plot close to these hypocenters, but 10 km deeper, and with the Rigo et al. (1996) model, it would be to the East, outside the frame of the Figure. With these same data of only the NOA array, but if ATH reading would be given the highest quality, computed hypocenters are all 10 to 17 km deeper than the best estimate of Bernard et al. (1997) and the epicenters plot in the Figure as N with the new model, O for the NOA model and R for the Rigo et al. (1996) model.

international and national agencies, or hypocenters obtained by other models, like hypocenters 1 and 2. Another important result is that hypocenters N1, N2, and N3 are rather close to each other, whereas they correspond to successive merging of different datasets. Hence, the use of the correct average model and Moho depth derived from a controlled source seismic experiment (Zelt et al., 2005) and of station terms derived from structural studies does a better job in terms of improving routine location. Unfortunately, however the

extensive tests show that this should be considered as only marginally significant, the stability of solutions reflecting the limited distribution of stations in azimuth and distance.

## 6. Conclusions

The estimates of earthquake locations obtained from regional networks using Pg and Pn data, trade off the resulting focal depth estimation with the assumed in the

velocity model Moho depth. The sparse permanent station distribution limits the reliability and spatial resolution due to uncompensated structural variation, mainly of Moho depth. Such structural variations can be estimated by dedicated seismic studies and then compensated in order to obtain more reliable and accurate hypocenter estimates.

Zelt et al. (2005) used tomographic inversion of PmP reflections from a grid of MCS profiles in the Gulf of Corinth recorded at several tens of temporary stations over central Greece. Their study yielded the average absolute Moho depth and crustal velocity in the region of the Gulf of Corinth and resolved with a fine lateral resolution their spatial variations.

The 26 July 2001 Mw=6.4 Skyros earthquake in the Aegean Sea was recorded by chance by these temporary stations, the vessel's streamer, a tight land line of several tens of geophone spreads over 8 km long, as well as by the national array of broad-band stations of NOA, Athens and the PATNET monitoring array of the University of Patras. This allows another new approach to derive the spatial variation of Moho topography and crustal velocity. Over 40 waveforms were obtained that provide a homogeneous set of consistent Pn high-resolution relative time picks of first-arrival Moho-refractions. Regardless of the accuracy of epicentral coordinates, depth and origin time, these yield high-resolution relative Pn time-terms to these stations.

First-order Moho depth variation can be tentatively derived from these Pn time-terms under the assumptions of regionally constant average crust and mantle velocities. Tying them in with the map of the absolute Moho depths obtained from EWING shots allows us to expand the sampled area over the whole central Greece. This documents a large Moho depth under the Hellenides belt and a shallower Moho domain towards the Aegean Sea, south and east of the Corinth Gulf. This shallow Moho domain is limited along a NE–SW prolongation ahead of the North Anatolian Fault, from the North Aegean Trough to the western tip of the Gulf of Corinth, suggesting a perturbation at depth within the lithosphere ahead of the North Anatolian Fault not seen with continuity in the surface geology.

The Pn time-terms, even under the simplifying assumption of an average velocity–depth model through the whole region, provide station corrections that compensate for the first-order structural heterogeneity. Relocation in this way of the 1995 Aigion earthquake with data from the sparse permanent monitoring stations shifts the hypocentral parameters closer to those derived from a dense local array (Bernard et al., 1997) implying improvement of the routine location.

## Acknowledgments

## References

Bernard, P., Meyer, B., Lyon-Caen, H., Gomez, J.-M., Tiberi, C., Berge, C., Cattin, R., Hatzfeld, D., Lachet, C., Lebrun, B., Deschamps, A., Courboulex, F., Larroque, C., Rigo, A., Massonnet, D., Papadimitriou, P., Kassaras, J., Diagourtas, D., Makropoulos, K., Veis, G., Papazisi, E., Mitsakaki, C., Karakostas, V., Papadimitriou, E., Papanastassiou, D., Chouliaras, G., Stavrakakis, G., 1997. The Ms=6.2, June 15, 1995 Aigion earthquake (Greece): evidence for low-angle normal faulting in the Corinth rift. J. Seismol. 1, 131–150.

Clément, C., Hirn, A., Charvis, Ph., Sachpazi, M., Marnelis, F., 2000. Seismic structure and the active Hellenic subduction in the Ionian Islands. Tectonophysics 329, 141–156.

Clément, C., Sachpazi, M., Charvis, P., Graindorge, D., Laigle, M., Hirn, A., Zafiropoulos, G., 2004. Reflection–refraction seismics in the Gulf of Corinth: hints at deep structure and control of the deep marine basin. Tectonophysics 391, 85–95.

Ganas, A., Drakatos, G., Pavlides, S.B., Stavrakakis, G.N., Ziazia, M., Sokos, E., Karastathis, V.K., 2005. The 2001 Mw=6.4 Skyros earthquake, conjugate strike-slip faulting and spatial variation in stress within the central Aegean Sea. J. Geodyn. 39, 61–77.

Hirn, A., Sachpazi, M., Siliqi, R., Mc Bride, J., Marnelis, M., the STREAMERS/PROFILES group, 1996. A traverse of the Ionian Islands front with coincident normal incidence and wide-angle seismics. Tectonophysics 264, 35–49.

Karagianni, E.E., Papazachos, C.B., Panagiotopoulos, D.G., Suhadolc, P., Vuan, A., Panza, G.F., 2005. Shear velocity structure of the Aegean area obtained by inversion of Rayleigh waves. Geophys. J. Int. 160, 127–143.

McKenzie, D., 1972. Active tectonics of the Mediterranean region. Geophys. J. R. Astron. Soc. 30, 109–185.

Makris, J., 1978. The crust and upper mantle of the Aegean region from deep seismic soundings. Tectonophysics 46, 269–284.

Mohorovičić, A., 1910. Das Beben vom 8. 10. 1909. Jahrb. Meteorol. Obs. Zagreb für 1909, Band 9, Teil 4, Abschn. 1.

Panagiotopoulos, D.G., Papazachos, B.C., 1985. Travel times of Pn-waves in the Aegean and surrounding area. Geophys. J. R. Astron. Soc. 80, 165–176.

Papadopoulos, T., Wyss, M., Schmerge, D.L., 1988. Earthquake locations in the western Hellenic Arc relative to the plate boundary. Bull. Seismol. Soc. Am. 78, 1222–1231.

Papadopoulos, G.A., Ganas, A., Plessa, A., 2002. The Skyros earthquake (Mw 6.5) of 26 July 2001, and precursory seismicity pattern in the North Aegean sea. Bull. Seismol. Soc. Am. 92, 1141–1145.

Papazachos, C., Nolet, G., 1997. P and S deep velocity structure of the Hellenic area obtained by robust nonlinear inversion of travel times. J. Geophys. Res. 102, 8349–8367.

Rigo, A., Lyon-Caen, H., Armijo, R., Deschamps, A., Hatzfeld, D., Makropoulos, D., Papadimitriou, P., Kassaras, I., 1996. A microseismic study in the western part of the Gulf of Corinth (Greece): implications for large-scale normal faulting mechanisms. Geophys. J. Int. 126, 663–688.

Sachpazi, M., Hirn, A., Avedik, F., Nercessian, A., McBride, J., Loucouyannakis, M., the Streamers group, 1997. A first coincident normal incidence-wide angle approach to the extending Aegean crust. Tectonophysics 270, 301–312.

Sachpazi, M., Hirn, A., Clément, C., Laigle, M., Roussos, N., 2003. Evolution to fastest opening of the Gulf of Corinth continental rift from deep seismic profiles. Earth Planet. Sci. Lett. 216, 243–257.

Spakman, W., van der Lee, S., van der Hilst, R.D., 1993. Travel-time tomography of the European–Mediterranean mantle down to 1400 km. Phys. Earth Planet. Inter. 79, 3–74.

Taylor, B., Goodliffe, A.M., Weiss, J.R., Sachpazi, M., Hirn, A., Laigle, M., Stefatos, A., 2003. Detachment tectonics in the Gulf of Corinth rift. EGS–AGU–EUG Joint Assembly, Paper EAE03-A-07222.

Tiberi, C., Diament, M., Lyon-Caen, H., King, T., 2001. Moho topography beneath the Corinth Rift area (Greece) from inversion of gravity data. Geophys. J. Int. 145, 797–808.

Tselentis, G., Melis, N., Sokos, E., Papatsimpa, K., 1996. The Egion June 15, 1995 (6.2 Ml) earthquake, Western Greece. Pure Appl. Geophys. 147, 441–451.

Vigner, A., 2002. Images sismiques par réflexions verticale et grand-angle de la croûte en contexte extensif: les Cyclades et le Fossé Nord Egéen. PhD Thesis, IPG Paris, pp. 269.

Willmore, P.L., Bancroft, A.M., 1960. The time term approach to refraction seismology. Geophys. J. R. Astron. Soc. 3, 419–432.

Zelt, B.C., Taylor, B., Weiss, J., Goodliffe, A.M., Sachpazi, M., Hirn, A., 2004. Streamer tomography velocity models for the Gulf of Corinth and Gulf of Itea, Greece. Geophys. J. Int. 159, 333–346.

Zelt, B.C., Taylor, B., Sachpazi, M., Hirn, A., 2005. Crustal velocity and Moho structure beneath the Gulf of Corinth. Geophys. J. Int. 162, 257–268.